

Linear electro-optic effect for femtosecond laser pulses in linear chirped MgO:LiNbO₃ and its compensation for phase mismatch and group-velocity mismatch

Dongzhou Zhong (钟东洲)

School of information, Wuyi University, Jiangmen 529020, China

Corresponding author: 179979410@qq.com

Received September 26, 2013; accepted October 10, 2013; posted online February 26, 2014

For linear electrooptic (EO) effect of femtosecond laser pulses that propagates along the direction of non-optical axis in linear-chirped and periodically poled MgO:LiNbO₃ (LCPPLMN), we explore the compensation scheme for the phase mismatch and the group-velocity mismatch between the o- and e-light, and discuss the effect of the linear chirp parameter of the LCPPLMN on the waveform of the output o- and e-light. It is found that, for any input pulse duration, the phase mismatch and the group-velocity mismatch can be simultaneously compensated by the optimization of the linear chirp parameter. As a result, high conversion efficiency of linear EO effect can be performed. In addition, we discuss the influence of the linear chirp parameter on the temporal evolutions of the output o- and e-light pulse.

OCIS codes: 190.3270, 190.7110.

doi: 10.3788/COL201412.S11901.

With the rapid development of femtosecond laser technology^[1-4], femtosecond laser pulse has attracted considerable interest owing to its applications to ultrafast optical communication, ultrafast nonlinear effect, micro-nano-processing, high-density information storage, laser medical treatment and THz radiation^[5-13]. In the above-mentioned applications, the manipulation of polarization, phase and intensity is of importance. The linear EO effect is known as being a common and efficient method. For describing the linear EO effect of femtosecond laser pulse, we put forward the coupling-wave theory of linear EO effect for ultrashort laser pulse, and investigate the characteristic of the linear EO effect of ultrashort laser pulse in bulk LiNbO₃ crystal^[14]. It is found that the linear EO effect is limited to many factors, such as the phase mismatch (PM), the group-velocity mismatch (GVM), the group-velocity dispersion (GVD), and the first- and second- order refractive dispersions. These factors will limit the phase-matching bandwidth and decrease the effective interaction length of pulse and the crystal. As a result, the conversion efficiency of the linear EO effect is reduced, and the waveform of laser pulse is seriously distorted. To obtain high conversion efficiency and make the pulse shape to stay the same, the GVD and the first- and second-order refractive dispersion need to be compensated. Also, it is crucial that the PM and GVM between two polarization components are compensated simultaneously. For the GVD and the first- and second-order refractive dispersions, we perform their complete compensation by optical phase conjugate scheme in recent work^[15]. For the compensations of the PM and GVM, the simplest method is that input laser pulse propagates along the direction of the optical axis of the crystal, which is considered to be the special situations of the birefringence technique. It is known that the birefringence technique has several disadvantages as follows. It cannot apply to all transparent wavelengths of

the EO crystal, and the maximum electrooptic coefficient cannot be used to improve the EO performance, whereas the developing quasi-phase matching (QPM) technique can overcome the above-mentioned disadvantages^[16-20]. Recently, with the development of the wave-coupling theory of linear EO effect^[11,14-18,21,22], there has been increasing interest in the use of periodically poled lithium niobate (PPLN) with QPM capability for linear EO effect application^[17,21,22]. PPLN doped with magnesium oxide is an important EO material and potential candidate in an EO effect since it has a high electric field of more than 5 KV/mm for ferroelectric domain, and greatly improved resistance to photorefractive damage threshold^[23,24]. In addition, linear chirped-periodically poled MgO:LiNbO₃ (LCPPLMN), as one of linear chirped QPM gratings, has been used to broaden effect the acceptance bandwidth of the second-order nonlinear effects^[20] since it can provide the compensations for the PM and GVM simultaneously. As known to all, linear EO effect is considered as one of the second-order nonlinear effects. So, it is prospective that the PM and GVM can be compensated simultaneously in a linear EO effect of femtosecond laser pulses based on LCPPLMN. However, the physical mechanism of the compensation for the PM and GVM is unclear in the processing of the linear EO effect for femtosecond laser pulses. For this purpose, based on the wave-coupling theory^[14], we explore the compensation mechanism for the PM and GVM in non-axis direction of LCPPLMN. Also, we discuss the influence of the linear chirp parameter of the crystal on the conversion efficiency of the linear EO effect and the waveform of output laser pulses.

The schematic diagram of linear EO effect for femtosecond laser pulses in LCPPLMN crystal is given in Fig. 1, where the optic axis of the crystal is along the direction of the z-axis of the crystal and the applied electric field is along the direction of the y-axis of the crystal. A light pulse propagating along the direction

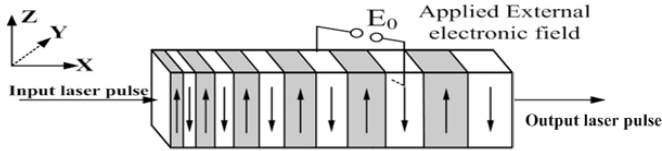


Fig. 1. The schematic diagram of linear EO effect for femtosecond laser pulses in LCPPLMN crystal.

of the x-axis of the LCPPLMN can be decomposed into two independent polarized components, i.e., o- and e- light. So the light field is

$$\mathbf{E}(t, x) = \frac{1}{2} \sum_{m=1}^2 \{ \mathbf{E}_m(t, x) \exp[i(\omega_0 t - k_m x)] \} + C.C, \quad (1)$$

where the subscript $m = 1$ and 2 denote the o- and e-light, respectively; \mathbf{E}_1 and \mathbf{E}_2 the slowly varying amplitude of the o-and e-light; ω_0 the central frequency of the laser pulse; $k_1 = 2\pi n_1/\lambda_0$ and $k_2 = 2\pi n_2/\lambda_0$ are the wave vectors of two polarized components at ω_0 , λ_0 the central wavelength; n_1 and n_2 the unperturbed refractive indices of two polarized components at the central frequency; $C.C$, complex conjugate. Besides, for one-dimension LCPPLMN crystal, its structure function is expanded by Fourier series, as follows:

$$f(\xi) = \sum_{m=-\infty}^{+\infty} f_M \exp[i\varphi_M(\xi)], \quad (2)$$

where $\varphi_M(\xi) = \int_0^\xi k_M(u) du$, $k_M(\xi) = 2\pi M/A(\xi)$ is the M-order reciprocal, $A(\xi)$ is the poled period. The Fourier coefficient $f_M = [1 - \cos(2\pi MD) + i\sin(2\pi MD)]/(i\pi M)$ for $M \neq 0$, $f_0 = 2D - 1$ for $M = 0$. The duty ratio $D = t^+/ (t^+ + t^-)$, t^+ and t^- are the lengths of positive domain and that of negative domain, respectively. With an external electric field applied on LCPPLMN crystal, light pulse can undergo rich quadratic effects^[21]. For example, EO effect: ω_{1z} (o-light) \leftrightarrow ω_{1y} (e-light). Second harmonic generation (SHG) or parametric down conversion (PDC): $\omega_{1y} + \omega_{1y} \leftrightarrow \omega_{2y}$ (eee), $\omega_{1z} + \omega_{1y} \leftrightarrow \omega_{2y}$ (oee); $\omega_{1z} + \omega_{1z} \leftrightarrow \omega_{2y}$ (ooe); $\omega_{1y} + \omega_{1y} \leftrightarrow \omega_{2z}$ (eeo); $\omega_{1z} + \omega_{1z} \leftrightarrow \omega_{2z}$ (ooo). Here the first-order reciprocal ($M = 1$) is considered to be very near the phase mismatch between the o- and e-light in linear EO effect. The other order reciprocals do not play an important role in linear EO effect because of phase mismatch. So these terms are neglected. In the coordinate reference system of the crystal, $x = L/2$ (L , the crystal length) is considered as the reference point, where the reciprocal is fixed at K_0 . The K_0 is designed to compensate the phase mismatch for linear EO effect, i.e., $K_0 = k_1 - k_2$. In the case, the first-order reciprocal K_1 is form of

$$K_1 = [K_0 - D_p(x - L/2)], \quad (3)$$

where D_p is the chirp coefficient. From the poled period of the crystal $A = 2\pi/K_1$, we have

$$\Lambda = \Lambda_0 [1 + \gamma(x - L/2)/L], \quad (4)$$

where $\Lambda_0 = 2\pi/K_0$, $\gamma = LD_p/K_0$ is the chirp parameter^[22], $k_0 = 2\pi/\lambda_0$. For different chirp parameter γ , we calculate the dependence of the first-order reciprocal K_1 on the location of the reciprocal K_1 . The related results are displayed in Fig. 2, where the related parameter values are given in Table.1. From Fig. 2, one sees that the K_1 decreases linearly with x (the location of the K_1). With $\lambda = 0.1$ and $x = 0$, the maximum K_1 ($K_{1\max}$) is $7.2 \times 10^5 m^{-1}$. However, for SHG and PDC cases, such as eee, oee, eeo, oeo, ooo, ooe and oee, all their wave vector mismatches are much larger than the $K_{1\max}$ (see Fig. 2), i.e., the phase mismatches in SHG or PDC effect cannot be compensated by the first-order reciprocal K_1 . So, with the range of γ from 0 to 0.2, SHG and PDC do not play an important role and are neglected because of phase mismatch. In the case, only linear EO effect in LCPPLMN crystal is considered. Let

$\mathbf{E}_1(t, z) = \mathbf{a}_1 \sqrt{\omega_0/n_1} A_1(t, z)$, $\mathbf{E}_2(t, z) = \mathbf{a}_2 \sqrt{\omega_0/n_2} A_2(t, z)$ and $\mathbf{E}_0 = \mathbf{c} E_0$, where \mathbf{a}_1 , \mathbf{a}_2 and \mathbf{c} are unit vectors. And suppose that the light pulse meets with plane-wave approximation, and the absorption loss of the crystal is neglected, we obtain the coupling-wave equations of linear EO effect for femtosecond laser pulses in a new coordinate reference system $\xi = |\beta_{21}|x/T_0^2$ and $\tau = t/T_0 - \beta x_0/T_0$, as follows:

$$\begin{aligned} & i(r_{11} \frac{\partial^2 A_1(\tau, \xi)}{\partial \xi^2} - r_{12} \frac{\partial^2 A_1(\tau, \xi)}{\partial \tau \partial \xi}) - i(G_1 - d_{22}) \frac{\partial^2 A_1(\tau, \xi)}{\partial \tau^2} \\ & + \frac{\partial A_1(\tau, \xi)}{\partial \xi} - (\frac{1}{L_T} + d_{21}) \frac{\partial A_1(\tau, \xi)}{\partial \tau} \\ & = [id_{10} A_2(\tau, \xi) + d_{11} \frac{\partial A_2(\tau, \xi)}{\partial \tau} + id_{12} \frac{\partial A_2(\tau, \xi)}{\partial \tau}] \\ & \exp[i\delta k \xi - i\varphi(\xi)] \\ & + id_{20} A_1(\tau, \xi) - i[\ell_1 |A_1(\tau, \xi)| + 2\ell_2 |A_2(\tau, \xi)|] A_1(\tau, \xi), \quad (5) \end{aligned}$$

$$\begin{aligned} & i(r_{12} \frac{\partial^2 A_2(\tau, \xi)}{\partial \xi^2} - r_{22} \frac{\partial^2 A_2(\tau, \xi)}{\partial \tau \partial \xi}) - i(G_2 - d_{42}) \frac{\partial^2 A_2(\tau, \xi)}{\partial \tau^2} \\ & + \frac{\partial A_2(\tau, \xi)}{\partial \xi} + (\frac{1}{L_T} - d_{41}) \frac{\partial A_2(\tau, \xi)}{\partial \tau} \\ & = [id_{30} A_1(\tau, \xi) + d_{31} \frac{\partial A_1(\tau, \xi)}{\partial \tau} + id_{32} \frac{\partial A_1(\tau, \xi)}{\partial \tau}] \\ & \exp[-i\delta k \xi - i\varphi(\xi)] \\ & + id_{40} A_1(\tau, \xi) - i[\ell_3 |A_2(\tau, \xi)|^2 + 2\ell_4 |A_1(\tau, \xi)|] A_2(\tau, \xi), \quad (6) \end{aligned}$$

where the normalized variables are used; the normalized phase mismatch $\delta k = T_0^2 \Delta k / |\beta_{21}|$, $\Delta k = k_1 - k_2$ is the phase mismatch between o-light and e-light; T_0 is the half-width at 1/e-intensity of input light pulse; $\beta_{21} = d^2 k_1(\omega) / d\omega^2|_{\omega=\omega_0}$ is the second-order group-velocity dispersion of the o-light pulse. The normalized walk-off length $L_T = |\beta_{21}| / [T_0(\beta_{12} - \beta_{11})]$, $\beta_{11} = dk_1(\omega)$

Table 1. The Parameter Values of the System for Calculation

Parameter	Symbol and value
The length of the crystal	$L = 15\text{mm}$
The reciprocal located in $x = L/2$	$K_0 = K_1 - K_2 = 3.199 \times 10^5\text{m}^{-1}$
The refractive index of o-light	$n_1 = 2.1726$
The refractive index of e-light	$n_2 = 2.093$
The center wavelength of input pulse (the corresponding frequency)	$\lambda_0 = 1550\text{nm}$ ($\omega_0 = 1.2161 \times 10^{15}$)
The electro-optic coefficients of the crystal	$r_{22} = 3.4$, $r_{23} = 8.6$, $r_{33} = 30.8$, and $r_{51} = 28$ (in 10^{-12}m/V)
The tensor elements of the third-order susceptibility of the crystal	$\chi_{12} = 1.12$, $\chi_{14} = 1$, $\chi_{33} = 9$, $\chi_{23} = 0.8$ (in $10^{-21}\text{m}^2/\text{V}^2$)
The azimuth angle	$\varphi = 0$
The polarization angle	$\theta = \pi/2$,
The light velocity in vacuum	$c = 3 \times 10^8\text{m/s}$
The dielectric permittivity susceptibility in vacuum	$\epsilon_0 = 8.854187818 \times 10^{-12}\text{F/m}$
The initial peak intensity of the pulse	$I_0 = 2\text{GW}/\text{cm}^2$
The duty ratio	$D = 0.5$
The first-order group-velocity dispersion parameter of o-light	$\beta_{11} = 7.4162 \text{ ns/m}$
The first-order group-velocity dispersion parameter of e-light	$\beta_{12} = 7.1223 \text{ ns/m}$
The GVD parameter of o-light	$\beta_{21} = 37.097 \text{ ps}^2/\text{km}$
The GVD parameter of e-light	$\beta_{22} = 47.874 \text{ ps}^2/\text{km}$
The initial and normalized chirp parameter of the pulse	$C_1 = 0$

$d\omega|_{\omega=\omega_0}$ and $\beta_{12} = dk_2(\omega)/d\omega|_{\omega=\omega_0}$ are the first-order group-velocity dispersion parameters of the o- and e-light, respectively. The normalized coefficients: $r_{11} = |\beta_{21}|/(T_0^2 k_1)$; $r_{12} = \beta_{11}/T_0 k_1$; $r_{21} = |\beta_{21}|/(T_0^2 k_2)$; $r_{22} = \beta_{11}/T_0 k_2$; $G_1 = (\beta_{11}^2 + 2k_1\beta_{21} - \beta_0^2)/(2k_1|\beta_{21}|)$ and $G_2 = (\beta_{12}^2 + 2k_2\beta_{22} - \beta_0^2)/(2k_2|\beta_{22}|)$ are the normalized and effective GVD parameters. $\beta_{22} = d^2k_2(\omega)/d\omega^2|_{\omega=\omega_0}$ is the second-order group-velocity dispersion of the e-light pulse, $\beta_0 = (\beta_{11} + \beta_{12})/2$. The normalized self-phase modulation coefficients are: $\ell_1 = 3T_0^2 k_0 \omega_0 R_{\text{eff}1} / (8|\beta_{21}|n_1^2)$; $\ell_3 = 3T_0^2 k_0 \omega_0 R_{\text{eff}3} / (8|\beta_{21}|n_2^2)$;

The normalized cross-phase modulation coefficients are: $\ell_2 = 3T_0^2 k_0 \omega_0 R_{\text{eff}2} / (8|\beta_{21}|n_1^2)$ and $\ell_4 = 3k_0 \omega_0 R_{\text{eff}2} / 8n_2^2$.

The effective third-order nonlinear coefficients are of forms $R_{\text{eff}1} = \sum_{ijkl} \chi_{ijkl} a_i a_j a_k a_l$ ($\{i, j, k, l\} = \{1, 2, 3\}$, the same

below), $R_{\text{eff}2} = \sum_{ijkl} \chi_{ijkl} a_i a_j b_k b_l$ and $R_{\text{eff}3} = \sum_{ijkl} \chi_{ijkl} b_i b_j b_k b_l$,

where χ_{ijkl} are the tensor elements of third-order susceptibility of LCPPLMN crystal. The normalized d-coefficients are of forms as

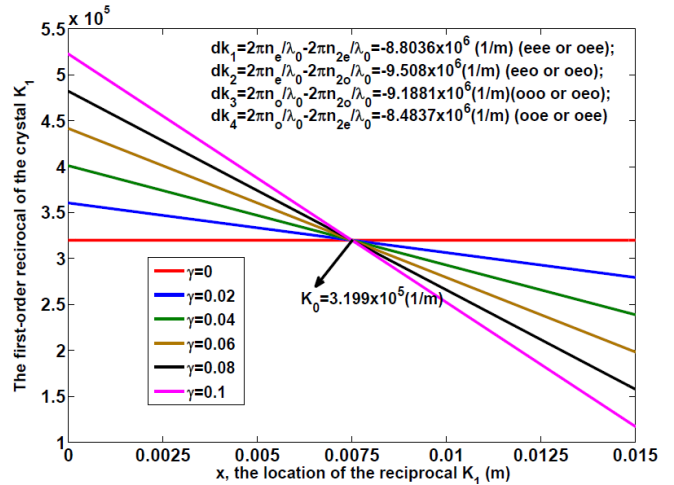


Fig. 2. (Color Online) For different chirp parameter γ , the dependence of the first-order reciprocal of the crystal K_1 the location of the reciprocal K_1 .

$$d_{1q} = \frac{k_0 E_0 T_0^{2-q}}{2|\beta_{21}|\sqrt{n_1 n_2}} f_1 \sum_{j=0}^q \frac{r_{\text{eff}1}^{(q-j)}}{\omega_0^j} + S_c \frac{r_{\text{eff}1}^{(q-1)}}{\omega_0},$$

($q = 0, 1, 2$, the same below) (7)

$$d_{2q} = \frac{k_0 E_0 T_0^{2-q}}{2|\beta_{21}|n_1} f_0 \sum_{j=0}^q \frac{r^{(q-j)}_{\text{eff}2}}{\omega_0^j} + S_c \frac{r^{(q-1)}_{\text{eff}2}}{\omega_0}, \quad (8)$$

$$d_{3q} = d_{1q}, \quad (9)$$

$$d_{4q} = \frac{k_0 E_0}{2n_2} f_0 \sum_{j=0}^q \frac{r^{(q-j)}_{\text{eff}3}}{\omega_0^j} + S_c \frac{r^{(q-1)}_{\text{eff}3}}{\omega_0}, \quad (10)$$

where $S_c = 0$ for $q = 0$, while $S_c = 1$ for $q = 1$ and 2 ; $f_0 = 2D - 1$ and $f_1 = [1 - \cos(2\pi D) + i\sin(2\pi D) + i\sin(2\pi D)]/(i\pi)$ are the zero- and first-order Fourier coefficients, respectively; The EO coefficients of $r^{(0)}_{\text{eff}j}$ ($j = 1, 2, 3$) are the same as those of $r_{\text{eff}j}$ ($j = 1, 2, 3$) in the Ref [17]; $r^{(1)}_{\text{eff}j}$ and $r^{(2)}_{\text{eff}j}$ are the first- and second-order derivatives of $r^{(0)}_{\text{eff}j}$ at ω_0 ; d_{1q} and d_{3q} describe the strength of EO coupling between two polarization components of light pulse; d_{2q} and d_{4q} result in the phase delays of these two polarization components, respectively. According to the phase $\varphi_1(\xi) = \int_0^\xi K'_1(u)du$ ($K'_1 = K_1 T_0^2 / \beta_{21}$), we have

$$\varphi_1(\xi) = T_0^2 [K_0(\xi - L/2) - D_p(\xi - L/2)^2 / 2] / |\beta_{21}|. \quad (11)$$

Let $A_1(\tau, \xi) = a_1(\tau, \xi) \exp\{i[\delta k\xi + \varphi_1(\xi)]/2\}$ and $A_2(\tau, \xi) = a_2(\tau, \xi) \exp\{-i[\delta k\xi + \varphi_1(\xi)]/2\}$; from Eqs (5)–(6), we obtain the coupling-wave equations of linear EO effect in frequency domain, as follows:

$$\begin{aligned} i r_{11} \frac{\partial^2 a_1(\Omega, \xi')}{\partial \xi'^2} + (r_{11} D_p \xi' + 1 + \Omega r_{12}) \frac{\partial a_1(\Omega, \xi')}{\partial \xi'} \\ - i[-\Omega(\frac{D_p \xi' r_{12}}{2} - d_{21}) + \Delta G(\Omega, \xi') + \frac{D_p \xi'^2}{4} r_{11} \\ + d_{20} + \Omega^2(G_1 - d_{22})] a_1(\Omega, \xi') + r_{11} D_p a_1(\Omega, \xi') / 2 \\ = -i[\ell_1 |a_1(\Omega, \xi')|^2 a_1(\Omega, \xi') \\ + 2\ell_2 |a_2(\Omega, \xi')|^2 a_1(\Omega, \xi')] + id_{10} a_2(\Omega, \xi') \\ + i\Omega d_{11} a_2(\Omega, \xi') - id_{12} \Omega^2 a_2(\Omega, \xi'), \end{aligned} \quad (12)$$

$$\begin{aligned} i r_{12} \frac{\partial^2 a_2(\Omega, \xi')}{\partial \xi'^2} + (-r_{12} D_p \xi' + 1 + \Omega r_{22}) \frac{\partial a_2(\Omega, \xi')}{\partial \xi'} \\ - i[\Omega(\frac{D_p \xi' r_{22}}{2} + d_{41}) - \Delta G(\Omega, \xi') + \frac{D_p \xi'^2}{4} r_{12} \\ + d_{40} - \Omega^2(G_2 - d_{42})] a_2(\Omega, \xi') - r_{12} D_p a_2(\Omega, \xi') / 2 \\ = -i[\ell_3 |a_2(\Omega, \xi')|^2 a_2(\Omega, \xi') \\ + 2\ell_4 |a_1(\Omega, \xi')|^2 a_2(\Omega, \xi')] + id_{30} a_1(\Omega, \xi') \\ + i\Omega d_{31} a_1(\Omega, \xi') - id_{32} \Omega^2 a_1(\Omega, \xi'), \end{aligned} \quad (13)$$

where $\xi = \xi - LT_0^2/(2|\beta_{21}|^2)$; $\Omega = \omega - \omega_0$; $\Delta G(\Omega, \xi) = \Omega/L_T + \gamma K_0 \xi/L$. The group-velocity mismatch can be compensated completely when $\Delta G(\Omega, \xi_{\text{pm}}) = 0$, where ξ_{pm} is the optimal dispersion compensation point.

For LCPPLMN crystal, the unit vectors of o- and e-light are of the forms of $\mathbf{a} = (\sin\varphi, -\cos\varphi, 0)$ and $\mathbf{b} = (-\cos\theta \cos\varphi, -\cos\theta \sin\varphi, \sin\theta)$, respectively. θ is the

polarization angle and φ is the azimuth angle. As shown in Fig. 1, $\theta = \pi/2$ and $\varphi = 0$ when light propagates along the direction of x-axis of the crystal, and we obtain $\mathbf{a} = (0, -1, 0)$ and $\mathbf{b} = (0, 1, 0)$. Besides, $\mathbf{c} = (0, 1, 0)$ because that the applied electric field \mathbf{E}_0 is along the y-axis of the crystal. Suppose further the input light pulse is a Gaussian one and comes only with the o-light component, i. e., $A_1(\tau, 0) = \sqrt{2I_0/c\epsilon_0\omega_0} \exp[-(1+iC_1)\tau^2/2]$ and $A_2 = (\tau, 0)$, where I_0 is the initial peak intensity of the pulse and C_1 is the initial and normalized chirp parameter of the pulse. In the following calculation, the parameter values of system are given in Table.1. The conversion efficiency of the linear EO effect is defined as

$$\eta = \int_{-\infty}^{\infty} I_2(\tau, L) d\tau / \int_{-\infty}^{\infty} [I_1(\tau, L) + I_2(\tau, L)] d\tau, \quad (14)$$

where

$$I_1(\tau, L) = c\epsilon_0\omega_0 |a_1(\tau, x)|^2 / 2,$$

$$I_2(\tau, L) = c\epsilon_0\omega_0 |a_2(\tau, L)|^2 / 2, \quad (15)$$

$$a_{1,2}(\tau, L) = \int_{-\infty}^{\infty} a_{1,2}(\Omega, L) \exp(i\Omega\tau) d\Omega / 2\pi. \quad (16)$$

For different input durations, Fig. 3 gives the dependence of the conversion efficiency η on the crystal length L , where E_0 is fixed at 3 KV/mm. From Fig. 3(a), it is found that, in the case of $T_0 = 5$ fs, the maximum η_{max} is 80% when $0.03 \leq \gamma \leq 0.05$; with T_0 increasing to 20fs, it becomes 90% when the γ is between 0.015 and 0.04; for $T_0 = 50$ fs, it can achieve 100% when the γ varies from 0.005 to 0.02. For different chirp parameter γ , Fig. 4 displays the dependence of the conversion efficiency η on the crystal length L . As seen from Fig. 4, the maximum conversion efficiency η_{max} is inversely proportional to the γ , and the optimal point x_{pm} becomes smaller with the η decreasing further. For example, from Fig. 4(a), one sees that, in the case of $T_0 = 5$ fs, the maximum conversion efficiency η_{max} locates at $x_{\text{pm}} = 15$ mm for $\gamma = 0.04$, and $\eta_{\text{max}} = 75\%$. With the γ fixed at 0.2, η_{max} is 28% at $x_{\text{pm}} = 9.2$ mm. If input duration T_0 is considered to increase further, η_{max} locates smaller x_{pm} . For example, for $\gamma = 0.04$, when T_0 is increased to 10 fs, 20 fs and 30 fs in turn, η_{max} is at 13mm, 11mm and 9mm in turn [see Fig. 4(b)–(c)]. From Fig. 4, it is further found that the conversion efficiency η is independent of the crystal length when $L > x_{\text{pm}}$. These results show that the conversion efficiency η heavily depends on the chirp parameter γ . By optimizing the value of the γ , high conversion efficiency η can be performed. The above-discussed results are obtained in the case of $E_0 = 3$ KV/mm. In the following, with T_0 fixed at 5 fs, we calculate the dependence of the η on the applied electric field E_0 for different γ ; the related results is displayed

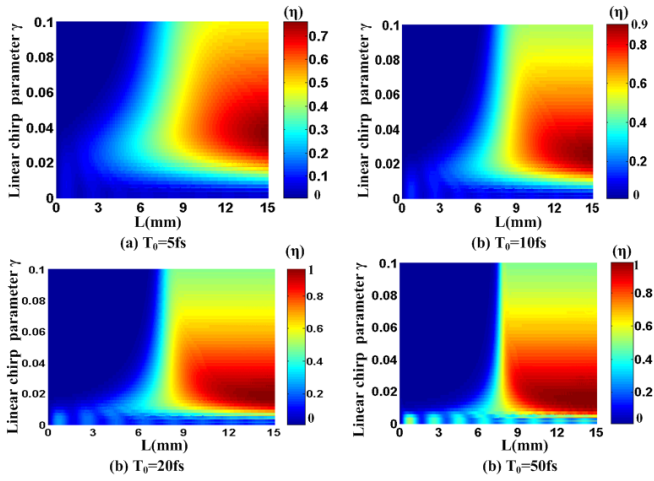


Fig. 3. (Color Online) The dependence of the conversion efficiency η on the chirp parameter γ and the crystal length L for different input durations, where E_0 is fixed at 3 KV/mm.

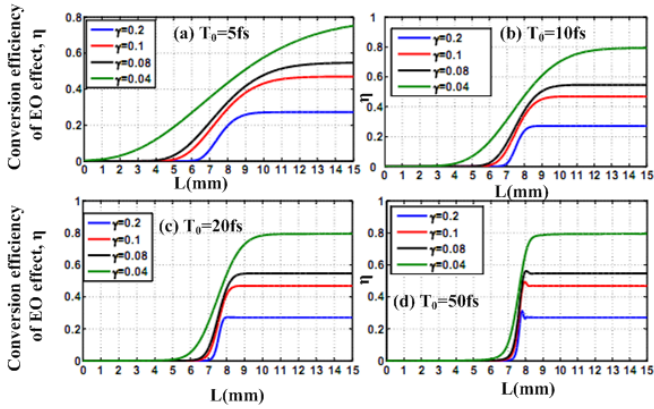


Fig. 4. (Color Online) For several fixed chirp parameter γ the dependence of the conversion efficiency η on the crystal length L in the case of different input duration T_0 .

in Fig. 5. As shown from Fig. 5, the η increases almost with the applied electric field E_0 when $0.08 \leq \gamma \leq 0.2$. If the γ decreases to 0.04, the η increases almost linearly with the E_0 which varies from 0 to 4kv/mm. But the η is almost independent of the E_0 when $E_0 > 4kv/mm$. From Fig. 5, one sees further that, for $\gamma = 0.04$, the increased rate of the η with the E_0 is the maximum; but for $\gamma = 0.2$, it is the minimum. These results show that the influence of the applied electric field on the conversion efficiency is limited to the chirp parameter of the crystal, owing to the compensation for the group-velocity mismatch depends heavily on the chirp parameter. In other words, from Figs. (3)–(5), it is concluded that the linear EO effect does not only depend the applied electric field and the crystal length, but also mainly depends on the chirp parameter. Besides, the chirp parameter influences seriously the temporal evolutions of the output o- and e-light pulses, as displayed in Fig. 6. From Fig. 6(a),

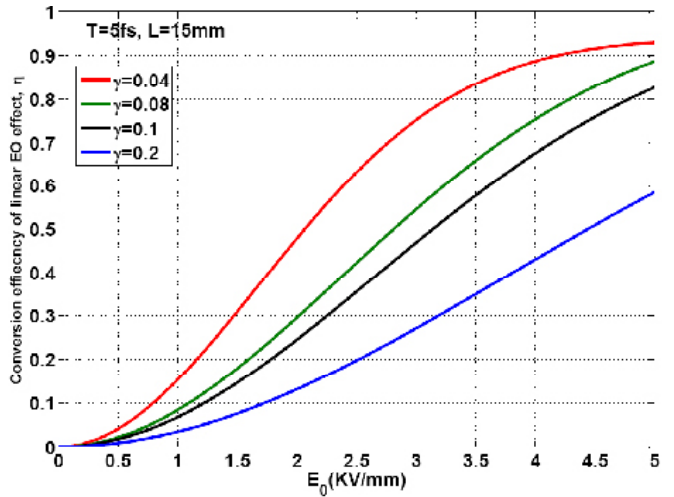


Fig. 5. (Color Online) For different the chirp parameter γ , the dependence of the conversion efficiency η on the applied electric field E_0 , where $L = 15$ mm and $T_0 = 5$ fs.

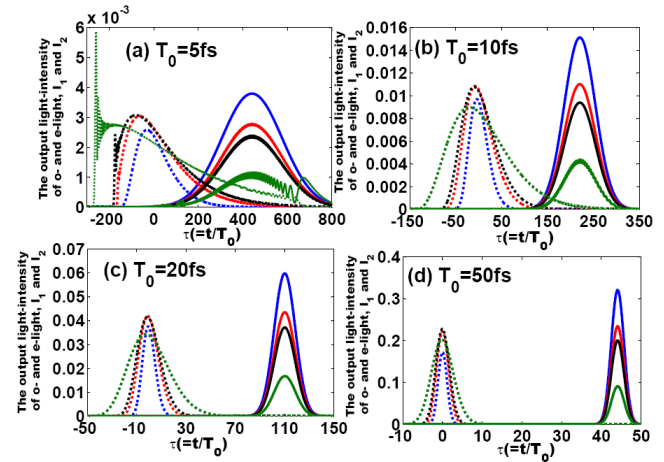


Fig. 6. (Color Online) For different input duration T_0 , the temporal evolution of the output o- and e-light pulse in the case of different chirp parameter γ , where the solid-line: the output o-light pulse; the dotted-line: the output e-light pulse; the blue line: $\gamma = 0.2$; the red line: $\gamma = 0.1$; the black line: $\gamma = 0.08$; the green line: $\gamma = 0.04$.

one sees that, for any γ , the output durations of the o- and e- light pulses are broadened severely when T_0 is fixed at 5 fs. This is due to the evident effect of the effective GVD and first- and second- order refractive dispersions. With T_0 increasing further, the broadening degree of the output durations becomes the smaller [see Figs. 6 (b)–(d)], owing to the decrease of the effective GVD and first- and second- order refractive dispersions^[14]. However, the output durations of two polarization components are sensitive to the γ . The further decreased γ causes the broader output duration of the e-light and the narrower that of the o-light. For example, as seen from the green curve in Fig. 6(a), of all the durations of output e-light pulses, for $\gamma = 0.04$, the output duration is broadened severely, and becomes the largest, if $\gamma = 0.2$, it is the

smallest [see the blue curve in Fig. 6(a)]. By comparison, of all the duration of the output o-light pulses, with γ fixed at 0.04, the output duration becomes the smallest, but for $\gamma = 0.2$, it is the largest.

In conclusion, the conversion efficiency of linear EO effect is decreased seriously due to the PM and the GVM between the o- and e-light, and the output waveform is distorted by the group-velocity mismatch when light pulse propagates along the direction of the non-optic axis of EO crystal. To solve these problems, in this paper, we take LCPPLMN crystal as an example to explore the compensation scheme for the phase mismatch and the group-velocity mismatch. It is found that, for any input duration, the PM and the GVM can be compensated. Thereby, high conversion efficiency can be performed. In addition, the output durations of two polarization components are sensitive to the linear chirp parameter of the crystal. The further decreased linear chirp parameter results in the smaller output duration of the o-light pulse and the larger one of the e-light pulse. The results presented in this paper may have a potential application in EO switching, EO modulator and EO filter with femtosecond pulse.

The authors acknowledge the financial supports from the natural science foundation of Guangdong province (NO. S2011010006105) and the doctoral initial fund for scientific search of Wuyi university.

References

1. J. A. Valdmanis and R. L. Fork, *IEEE J. Quantum Electron.* **22**, 112 (1986).
2. R. L. Fork, C. H. B. Cruze, P. C. Becker, and C. V. Shank, *Opt. Lett.* **12**, 483 (1987).
3. A. Kasper, *Opt. Lett.* **21**, 743 (1996).
4. I. D. Jung, F. X. Kartner, N. Matuschek, D. H. Sutter, F. Morier-Genoud, G. Zhang, U. Keller, V. Scheuer, M. Tilsch, and T. Tschudi, *Opt. Lett.* **22**, 1009 (1997).
5. H. K. Eaton, Ph. D. dissertation (Colorado University, 1999).
6. J. Krieger and W. Kautek, *Laser Phys.* **9**, 30 (1999).
7. K. König, I. Riemann, P. Fischer, and K. J. Halbhuber, *Cell. Mol. Biol.* **45**, 195 (1999).
8. K. S. Layland, I. Riemann, U. A. Stock, and K. König, *J. Biol. Opt.* **10**, 0240171 (2005).
9. B. K. Ngoi, K. Venkatakrishnan, B. Tan, P. Stanley, and L. E. N. Lim, *Opt. Express* **9**, 200 (2001).
10. L. R. Chen, S. D. Benjamin, P. W. E. Smith, and J. E. Sipe, *IEEE J. Quantum Electron.* **34**, 2117 (1998).
11. Z. Zheng and A. M. Weiner, *Chem. Phys.* **267**, 161 (2001).
12. S. Döring, S. Richter, S. Nolte, and A. Tünnermann, *Opt. Express* **18**, 20395 (2010).
13. M. M. Wefers and K. A. Nelson, *Opt. Lett.* **18**, 2032 (1993).
14. D. Zhong and W. She, *Appl. Phys. B* **104**, 941 (2011).
15. D. Z. Zhong and W. She, *Acta. Phys. Sin.* **61**, 064214.1 (2012).
16. C. R. Phillips, J. S. Pelc, and M. M. Fejer, *Opt. Lett.* **36**, 2973 (2011).
17. G. L. Zheng, H. C. Wang, and W. L. She, *Opt. Express* **14**, 5535 (2007).
18. Wenguo Zhu and Weilong She, *Opt. Lett.* **37**, 2823 (2012).
19. C. R. Phillips, C. Langrock, J. S. Pelc, M. M. Fejer, J. Jiang, M.E. Fermann, and I. Hartl, *Opt. Lett.* **36**, 3912 (2011).
20. M. Charbonneau-Lefort, B. Afeyan, and M.M. Fejer, *J. Opt. Soc. Am. B.* **25**, 46 (2008).
21. D. Huang and W. L. She, *Opt. Express* **15**, 8275 (2007).
22. X. Q. Zeng, L. X. Cheng, H. B. Tang, D. Z. Zhong, and W. L. She, *Opt. Express* **18**, 5061 (2010).
23. Y. Furukawa, K. Kitamura, S. Takekawa, K. Niwa, and H. Hatanoto, *Opt. Lett.* **23**, 1892 (1998).
24. Y. L. Chen, J. Guo, X. J. Liu, C. Lou, J. W. Yuan, Y. F. Luo, J. J. Xu, and S. L. Chen, *Opt. Commun.* **238**, 201 (2004).